ACCURACY ANALYSIS FOR KOLMOGOROV ENTROPY USED IN STUDYING THE CHAOTIC DYNAMICS OF CFB REACTORS BASED ON SOLIDS CONCENTRATION FLUCTUATIONS

S. V. Manyele
Department of Chemical and Process Engineering
College of Engineering and Technology
University of Dar es Salaam, P.O. Box 35131, Date s Salaam
smanyele@cpe.udsm.ac.tz

ABSTARCT

A study on the chaotic dynamics of a high flux circulating fluidized bed (CFB) riser (10-m high and 76-mm i.d.) using the maximum likelihood estimate of the Kolmogorov entropy (K_{ML}) is reported. The signals used were measured by using a solids concentration fiber optic probe, accuracy of which is reported based on statistical analysis. The sensitivity analysis of the parameters used for computing K_{ML} was conducted to identify optimum settings, based on the standard error, $s(K_{ML})$ and the nature of PDF of the b-values from the reconstructed phase space trajectories. The length of time series, N, sampling frequency, f_s, and number of embedding dimensions, D_{im}, and $\bar{b}$, strongly affect the accuracy of K_{ML} values. A relationship between K_{ML} and $\bar{b}$ was established, which was obeyed by experimental data from all operating conditions studied, and for all sampling frequencies. The chaotic dynamics of the CFB was studied by examining the effect of increasing the local solids concentration at different axial elevations and different operating conditions in a high flux riser. It was concluded that the K_{ML} method is highly accurate when N > 3,000 data points, for which the effect of D_{im} is negligible and PDFs of the b-values becomes similar in shape based on $\sigma(b)$, $S_k(b)$ and $K_u(b)$.

Keywords: *Solids concentration fluctuations, accuracy of measurements, time series analysis, chaos analysis, Kolmogorov entropy.*

INTRODUCTION

Multiphase reactors exhibit complex non-linear oscillations (mixed periodic and chaotic oscillations). Moreover, the dynamics of such systems exhibit both spatial complexity (different dynamics from one location to another) and sometimes temporal complexity (different dynamics from one time to another) (Addison, 1997), especially due to feed variations and gas pulsations. This complexity has been studied using both one-dimensional approach (statistical and spectral analyses) and also a multi-dimensional approach using phase-space statistics (chaos analysis).

Chaos analysis is not the only tool for the analysis of the complex dynamics of multi-phase reactors; other methods include statistical analysis and spectral analysis. However, statistical analysis (using mean, standard deviation and properties of the PDF) does not keep track of time-dependency behavior of the multiphase reactors (van der Stappen *et al.*, 1993), i.e., even when the signal is arranged in ascending order of values, the same value is obtained. Chaos analysis has been used in the study of weather (Lorentz model), economics, epidemiology and ecology (Schaffer, 1985; Müller *et al.*, 1995), demography, and in medical diagnostics (Hoyer *et al.*, 1998). The analysis of multiphase dynamics using chaos analysis has been so far developed and used for analysis of pressure fluctuations (Manyele, *et al.*, 2002a; 2003), solids concentration signals (Cheng *et al.*, 1998), and temperature fluctuations.

In the analysis of solids concentration signals form a CFB, the mean value of the signal describes what is measured while standard deviation and other statistical measures represent noise and other interferences. In the CFB, such interferences are caused by gas flow pulsations and formation and breakdown of clusters (Manyele *et al.*, 2002b). Different from macroflow, the microflow studies are normally focused on quantifying the fluctuating component of the signal (Manyele *et al.*, 2003); however, the fluctuations must be within reasonable range (Soong *et al.*, 1994).

During solids concentration measurements in the CFB, the final state is regarded to be the steady state condition when all flows remain constant. Starting signal recording some time after the process has started attains the conditions of stationarity. However, the signals must still be tested for stationarity before chaos analysis can be applied (Finney *et al.*, 1996). The stationarity condition is attained when the statistical averages (i.e. mean, standard deviation) remain constant along different segments of the signal or time series.

In a CFB riser, for example, dilute and dense phase flow take place dominantly at the center and in the wall region and bottom section, respectively (Johnson and Johnson, 2001; Manyele *et al.*, 2002a). Chaos analysis has been able to distinguish such flows based on strong sensitivity of its parameters (correlation dimension and Kolmogorov entropy) (Bai *et al.*, 1999; Manyele *et al.*, 2002a; 2003; 2006). Similarly, the axial flow structure along the CFB, which varies widely (entrance, acceleration, transition and the exit sections), have been identified using chaos analysis of pressure fluctuations and solids concentration signals from high density risers (Manyele *et al.*, 2006; 2002a; Bai *et al.*, 1999) and downers (Cheng *et al.*, 1998; Manyele *et al.*, 2003).

The Kolmogorov entropy characterizes the sensitivity of the gas-solids flow to small disturbances and its rate of information loss; it is also a measure of the predictability of the changes in the gas-solids flow (Grassbeger and Procaccia, 1983; Daw, 1990; 1991; 1992). Higher entropy signifies higher rate of information loss (or lower predictability) and also stronger dependency on small disturbances. Recently, K_{ML} have been extensively used to study the chaotic behavior of CFB risers and downers based on both solids concentration data (Cheng *et al*., 1998; Manyele *et al.*, 2003; 2006).

The most acceptable algorithm for computation of Kolmogorov entropy is the maximum likelihood method developed by Schoulten *et al*. (1994), denoted as K_{ML}. However, the accuracy of the data processing technique for determination of K_{ML} depends on a number of parameters such as sampling frequency, length of the time series, time average solids concentration, and number of embedding dimensions used in phase space reconstruction. This paper analyzes the effect of these parameters using solids concentration data from CFBs. After establishing the optimum values for these parameters, the chaotic behavior of the CFB was studied by examining the effect of local solids concentration in a high flux riser. Moreover, the accuracy of the measurement technique for solids concentration fluctuations was analyzed using statistical methods.

EXPERIMENTAL DETAILS

The signals used in this study were measured in two different units: (a) one of the risers of a 10-m CFB twin-riser system, with 76-mm i.d. operated at high flux, and (b) from a downer reactor 100-mm diameter and 9.3 m tall, operated at low flux conditions. The solids circulating in each of these systems were spent FCC catalyst with a mean diameter of 67 μm and a particle density of 1500 kg/m^3. Figure 1 shows the setup of the two units. The riser was operated at high flux conditions (U_g = 5.5 to 10.0 m/s and G_s = 100 - 550 kg/m^{2}s, while the downer was operated under dilute conditions (U_g = 3.7 to 10.0 m/s and G_s = 50 to 200 kg/m^{2}s). The details of the two units have been reported by Manyele *et al*. (2003; 2006).

Solids concentration fluctuations measurements were conducted using a reflective-type optical fiber concentration-probe for both units. The active area in the probe tip was approximately 2 mm x 2 mm, consisting of approximately 8000 emitting and receiving quartz fibers, each having a diameter of 15 μm. More details of this probe including its calibration procedure can be found from Zhang *et al.* (1998). Measurements were taken on several axial levels and at several radial positions. The sampling time was 30 seconds at a frequency of 970 Hz. Each stored signal consisted of 27,000 data points. Data analysis was conducted using FORTAN codes.

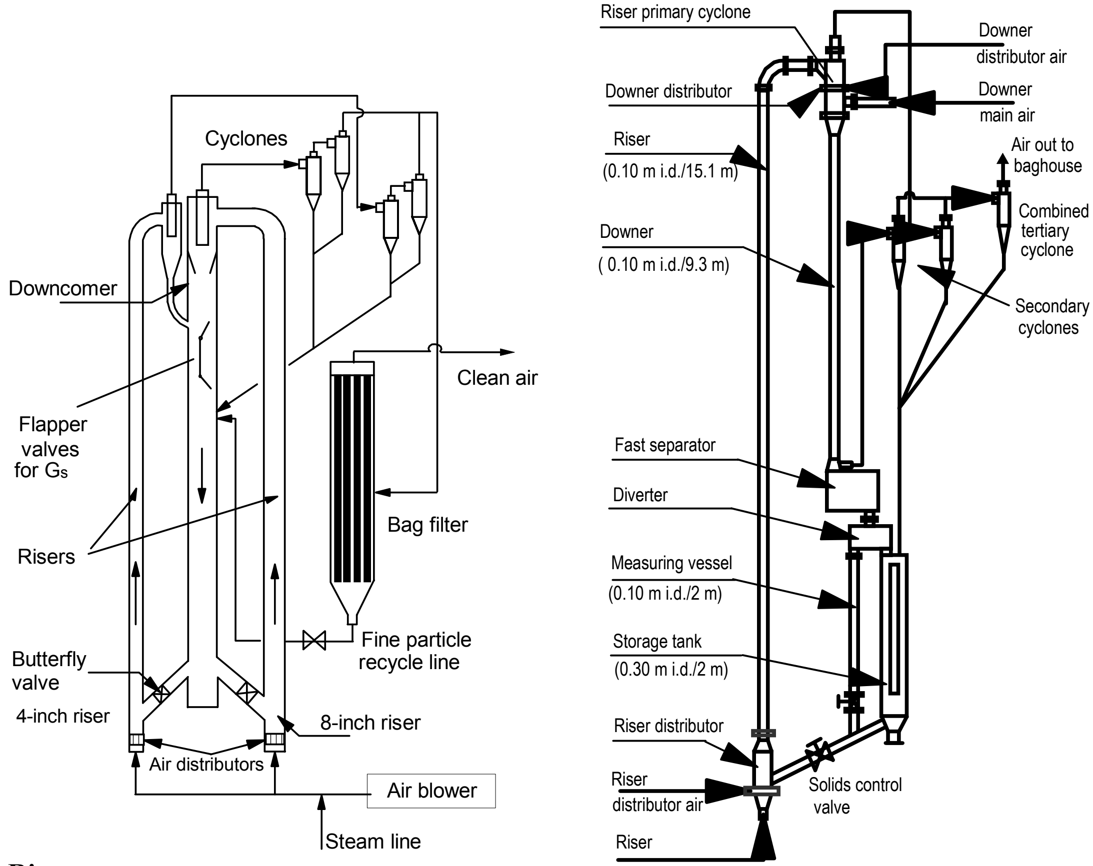

Riser **Downer**

Figure 1: Experimental setup for downer and riser CFBs

DETERMINATION OF KOLMOGOROV ENTROPY USING MAXIMUM LIKELIHOOD METHOD

The maximum likelihood approach was proposed for the estimation of Kolmogorov entropy of experimental data, K_{ML} (Schoulten *et al.*, 1994). Because the computations of the Kolmogorov entropy using the method of Grassberger and Proccaccia (1983) do not have a known standard error, the maximum likelihood method has gained acceptance in the multiphase reactor signal processing. However, this method needs analysis before it can be implemented. The accuracy of the computational results for K_{ML} depends on the following factors: the average value of *b*, the sampling frequency, the effect of the length of the time series used in the computation, and number of embedding dimensions used.

This maximum likelihood method is based on the average number of steps before the exponential divergence between reconstructed trajectories exceeds the average absolute deviation, *AAD*, of the original time series, using a time delay of one sampling interval, Δt, for phase space reconstruction, as shown in equation (1).

$$K_{ML} = -\frac{1}{\tau}\ln\left(1-\frac{1}{\bar{b}}\right) \qquad (1)$$

where $\bar{b}$ is the average number of steps before the distance between two points exceeds the *AAD* or the crossing distance, and $\tau = \Delta t$. A positive value of K_{ML} is a necessary condition for a system to be chaotic.

The average absolute deviation (*AAD*) is simply the average value of the departure of the instantaneous values of the solids concentration from the mean value (Schoulten and van den Bleek, 1998; Marzochella *et al.*, 1997; van der Stappen *et al.*, 1993b), expressed mathematically as per equation (2):

$$AAD = \frac{1}{N}\sum_{i=1}^{N}\left(\left|X_i - \overline{X}\right|\right) \qquad (2)$$

where *N* is number of data points in the signal and *X* is the one-dimensional series of solids concentration values.

RESULTS AND DISCUSSION

Accuracy of the Measurement System

The accuracy of measurements was expressed in terms of the coefficient of variation, CV (the ratio of the standard deviation to the mean), and signal to noise ratio, SNR (the ratio of the mean value to the standard deviation). A plot showing CV and SNR versus the time-averaged solids concentration, ε_s, for a wide range of operating conditions is shown in Figure 2 (using data from a downer reactor).

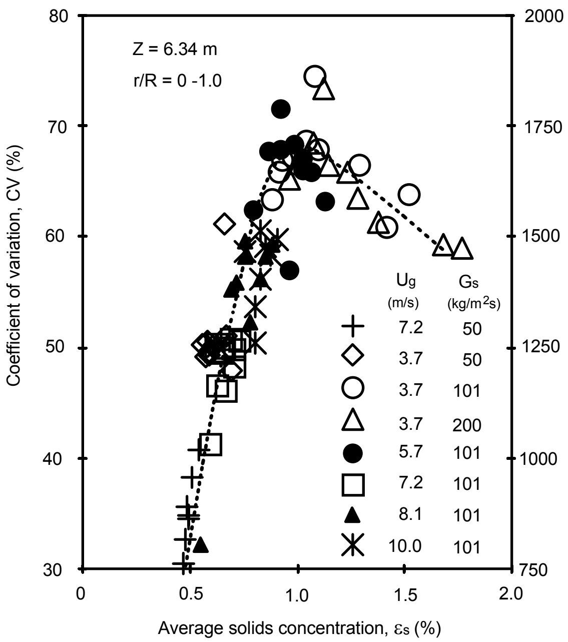

Figure 2: Variation of the coefficient of variation (CV) and signal-to-noise ratio (SNR) with the average solids concentration in the downer reactor (sample data from the fully developed section)

For ε_s less than 1.0%, *CV* increases faster reaching a maximum at $\varepsilon_s \approx 1.0\%$, before decreasing again as ε_s approaches 2.0%. The *CV* varied between 30 - 70% showing that the mean value is always higher than the fluctuations. The corresponding values of *SNR* range from 750 – 1750, which are sufficiently higher signifying that the noise component is smaller. Moreover, the variation of U_g and G_s has no significant difference on *CV* and *SNR*.

Accuracy of Skewness and Kurtosis used to analyze the Properties of PDFs

In this study, Skewness and Kurtosis were employed in analyzing the properties of the PDF of sampled solids concentration signals and also for the PDF of the counted number of points in phase space during computation of K_{ML}. High positive Skewness indicates that the PDF have a long tail towards higher values (to the right), while the Kurtosis measures the tendency of the PDF to have a high peak.

The accuracy of both S_k and K_u depend strongly on the number of samples used in computation, that is *N*. For the calculated values of Skewness and Kurtosis to be meaningful, the corresponding standard deviation as the estimators of both S_k and K_u of the underlying distribution, must be known.

For the ideal case of a normal (Gaussian) distribution, the standard deviation of the computed S_k as an estimator of the Skewness is approximately $S_{k,N} = \sqrt{15/N}$, which is equal to 0.024 for N = 27,000 used in this study. The accuracy of the computed Skewness is high when the computed value is many times as large as $S_{k,N}$. To examine the accuracy of the computed values of Skewness of the sampled signals, the values are plotted versus the time-averaged solids concentration, ε_s, as shown in Figure 3. The horizontal dashed line indicates a base line for $S_{k,N}$ = 0.024. The computed values of Skewness ranged from 1 to 10, which are clearly higher than 0.024, about 40 – 100 times, for all operating conditions. The Skewness also shows a maximum at ε_s = 1.0%, similar to *CV*.

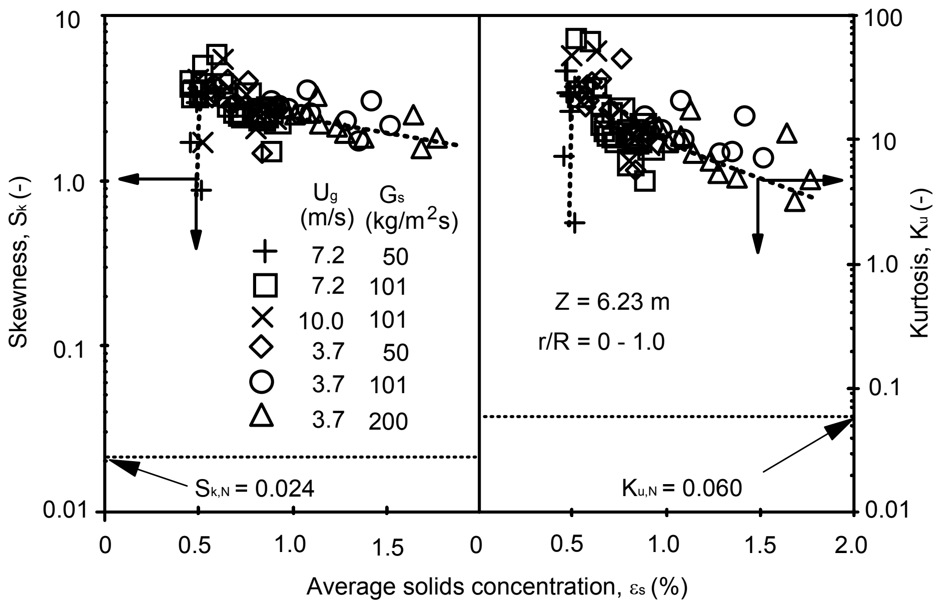

Figure 3: Range of values for both Skewness and Kurtosis in the downer reactor (sample data from the fully developed section).

Based on the normal (Gaussian) distribution, again the standard deviation of the Kurtosis as an estimator of the Kurtosis of the underlying distribution is given by $K_{u,N} = \sqrt{96/N}$. The same approach was used as for Skewness. The accuracy was inferred by comparing the computed values of K_u with the $K_{u,N}$. Figure 3 shows also the variation of K_u with ε_s for similar operating conditions. The K_u values range from 1 to 100 and are far higher than the $K_{u,N}$ = 0.060. Similarly, the Kurtosis shows a peak as ε_s is increased from 0.5 to 2.0%. The above analysis was then used to examine the PDFs of the b-values created from the reconstructed trajectories, with $N = 10^6$.

The effect of $\bar{b}$ of the Reconstructed Vector on the K_{ML}

Figure 4 shows the range of *b*-values for signal reconstructed using 100 embedding dimensions for N = 5000 data points. The determination of *b*-values requires counting of points on the attractor before the separation distance from a given arbitrary stationary point exceeds *AAD*. Once *AAD* is exceeded, the number of points counted is recorded. The computer is then instructed to jump to another arbitrary point on the attractor and the counting is repeated.

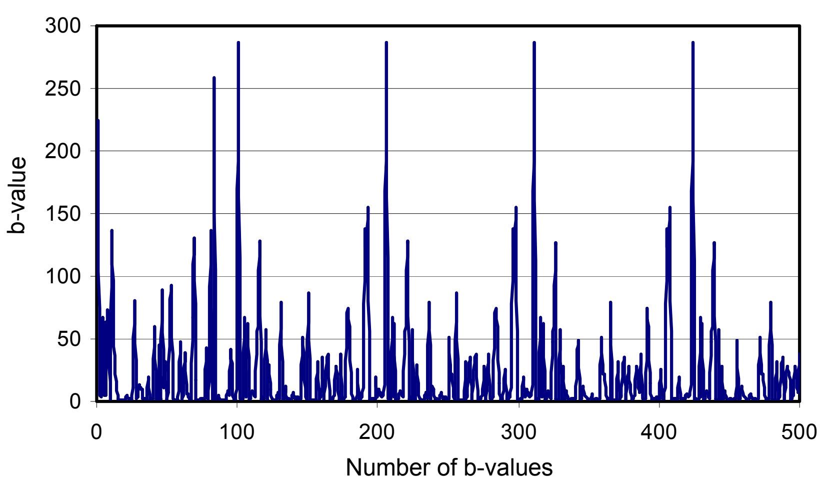

Figure 4: Range of *b*-values for a solids concentration signal embedded at D_{im} = 100 and N = 5,000 using a signal from a high flux riser (U_g = 8.0 m/s; G_s = 300 kg/m^{2}s; Z = 6.34 m and r/R = 0)

Using the maximum-likelihood method, several values of *b* are determined, the average of which is used to calculate the K_{ML}. With a large value of *M*, it is also interesting to examine the nature of the PDF. The sequence of values of *b* obtained from a given time series were used to study the probability distribution function (PDF). This was studied by computing the standard deviation and Skewness of the b-values as *N* changes, as shown in Figure 5. For $N < 1,000$ points, the effect of D_{im} is stronger leading to totally different shapes of PDFs for the b-values whenever D_{im} is changed, as observed from the wide variation in the standard deviation, $\sigma(b)$, Skewness, $S_k(b)$ and Kurtosis, $K_u(b)$. Meanwhile, the Skewness increases with *N* until it levels off for $N > 1,000$. With standard deviation between 6.0 and 8.0 (for $N > 1,000$), it shows that the values of *b* are relatively similar.

In the analysis of b-values, the Skewness was observed to range between 2.5 to 3.0 at higher *N*. Based on the accuracy analysis results from Figure 3, the experimental values are far higher than the $S_{k,N}$, signifying that the computed S_k values of the underlying PDF of *b*-values is highly accurate. The fact that the Skewness values for the PDF of *b*-values are far higher than the $S_{k,N}$ for the PDF of a normal distribution, i.e. 0.004 for $N = 10^6$ counts, signifies that the computed Skewness values are of high accuracy.

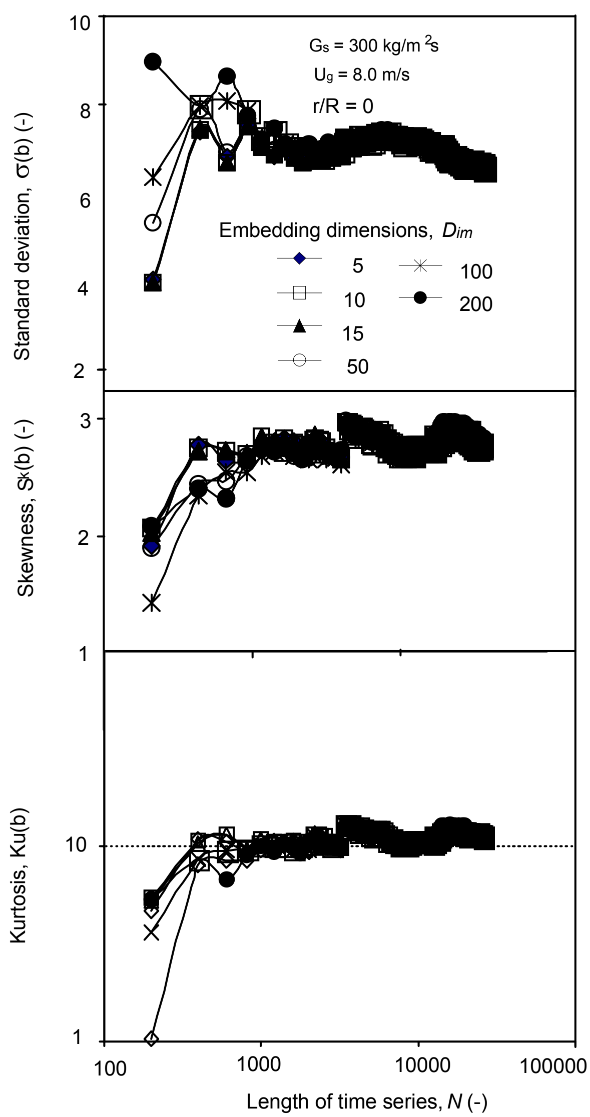

Figure 5: Effect of the time series length, *N,* on the nature of the PDF of *b*-values at different D_{im}

Effect of Sampling Frequency on K_{ML}

The fiber optic probe used for measurements of solids concentration was sampled at a frequency of 970 Hz. With such a fast sampling software and hardware combination, it was possible to reduce the frequency from 970 to 61 Hz, and study the effect of the sampling frequency. However, for accuracy, the highest frequency is preferred because it captures the dynamics to the maximum possible state. Figure 6 shows the effect of b value on the range of values of K_{ML} at different sampling frequencies. By changing the sampling frequency of the signal a different loci of the K_{ML} values is obtained.

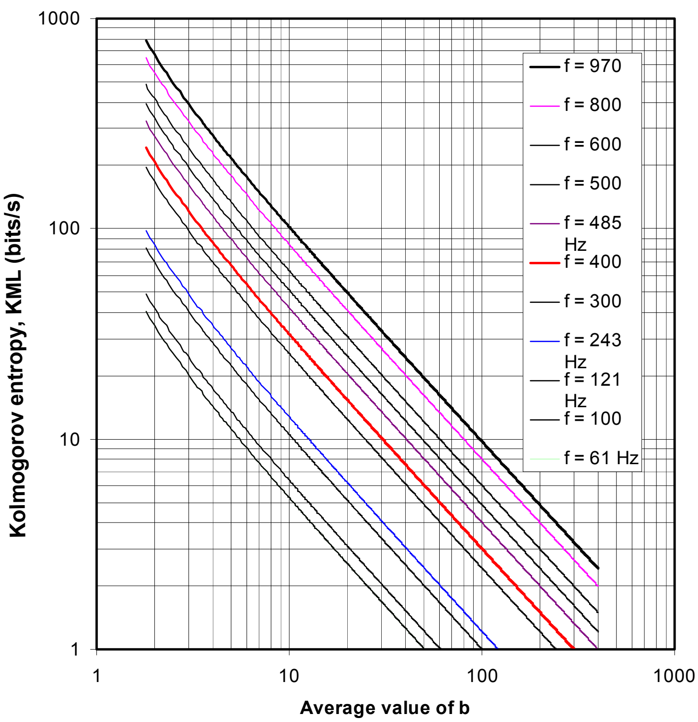

Figure 6: Variation of K_{ML} with the average b-value at different sampling frequencies for signals from a high flux riser (U_g = 8.0 m/s; G_s = 300 kg/m^{2}s; Z = 6.34 m and r/R = 0)

Figure 6 shows that the higher the frequency the higher the K_{ML} value. Thus, the same system sampled at a lower frequency will lead to lower values of K_{ML} and vice versa. However, because the locus gives a straight line on a log-log plot, the profiles in the CFB will be the same if the same equations are used. Figure 6 shows also that the higher the average value of b the lower the K_{ML} value. This is in accordance to the fact that since $\overline{b}$ gives the number of steps before the distance on the attractor exceeds *AAD*, then, lower value of $\overline{b}$ implies that the attractor is more sparsely populated by vector points, or the points are far apart, an indication of a large phase space, and that only a few points are encountered, before *AAD* is exceeded, implying a higher value of K_{ML}.

Figure 7 shows the variation of K_{ML} with $\overline{b}$ for signals sampled from the high flux riser t different operating conditions. A log-log plot gives a straight line for all conditions, which was fitted by a relationship:

$$K_{ML} \propto b^{-1.033} \qquad (3)$$

For all operating conditions studied, the relationship presented in equation (3) was observed. The experimental data follows this relationship for dilute and high density conditions, as G_s was changed from 100 to 550 kg/m^{2}s under the same gas velocity (8.0 m/s). Also, the change in velocity from 5.5 to 10.0 m/s at constant G_s of 300 kg/m^{2}s did not affect the relationship. As shown in Figure 6, a similar relationship will be obtained for all sampling frequencies.

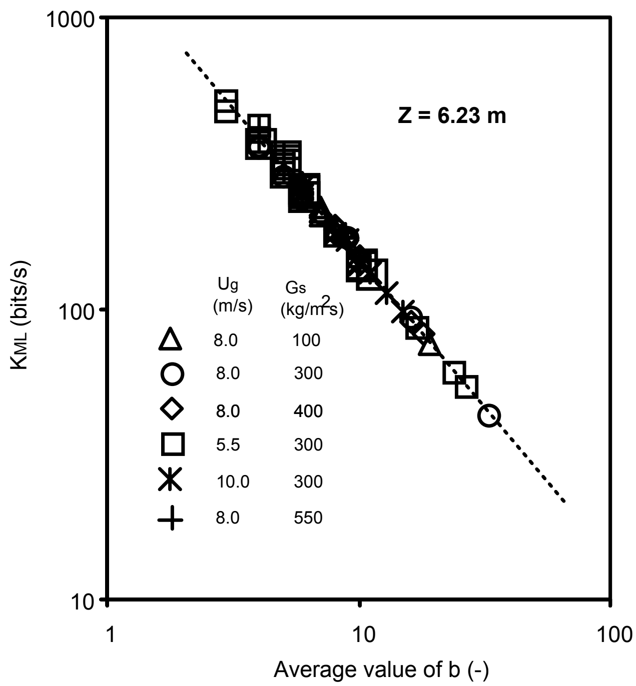

Figure 7: Variation of K_{ML} with b for different operating conditions in a high flux riser in the fully developed section

The effect of Time Series Length on the Actual value and Accuracy of K_{ML}

The length of the time series used in phase space reconstruction is determined by computation speed of the computer. To minimize the computation time, optimization can be done on the computer code or by changing the length of the time series, N. Figure 8 shows the semi-log plot of the variation of K_{ML} with N (200 – 27,000) for a wide range of embedding dimensions (D_{im} = 5 – 200) for a signal from a high-density riser.

For N < 1000 points, the K_{ML} varies widely with N without a clear pattern. However, for N > 1,000 points, all the values follow a single curve for all D_{im}. This shows that:

(a) The effect of D_{im} is strong for shorter time series than 1,000 pints.

(b) The accuracy and repeatability of K_{ML} values is higher for longer time series.

(c) For longer time series, any number of embedding dimensions will lead to the same range of K_{ML} values.

Schoulten *et al.* (1994) proposed the standard error for the computed values of K_{ML} to be $M^{-0.5}$, where M is the number of times the distances exceed the average absolute deviation of the signal (number of crossings, which is equal to the number of b-values). In this study, the optimization of the computation time was based on N for which the accuracy is reported as the former increases. Parallel to the computation of K_{ML}, the standard error values were also estimated. Figure 9 shows the log-log plot of the variation of the standard error of K_{ML} with the length of the time series used for the phase space reconstruction.

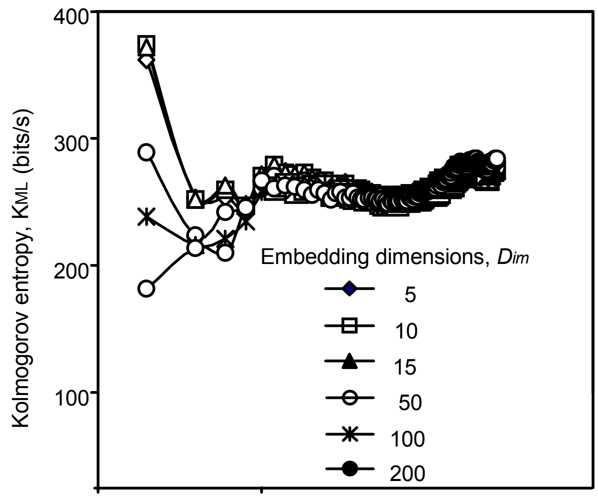

Figure 8: Effect of the time-series length on the K_{ML} values and the corresponding accuracy (based on the standard error values, signal from a high-density riser)

Below $N = 3{,}000$, the standard error in the estimate of K_{ML} is higher and decreases until $N = 3{,}000$, beyond which it remains constant at about 0.001. The same values of the standard error were obtained regardless of the number of embedding dimension. However, because $s(K_{ML})$ decreases for lower values of N, the best range of time series length is $N > 3{,}000$ points for higher accuracy. However, the number of embedding dimensions has no effect on the standard error. Therefore, to minimize computer time, a smaller $D_{im} = 5$ and N slightly above 3,000 can be used to estimate K_{ML} values.

It is important to determine the relative standard error of the K_{ML} (entropy estimate), $s(K_{ML})$. It is suggested that $s(K_{ML}) \leq 0.1\%$, i.e., K_{ML} values should be based on at least a sample size the order of 10^6 values of b. This counting is performed for a large number of times, about 10^6. The possibility of having such higher number of b values is based on the fact that the embedding dimensions leads to a length of the embedded signal of length = $(N)^{Dim}$.

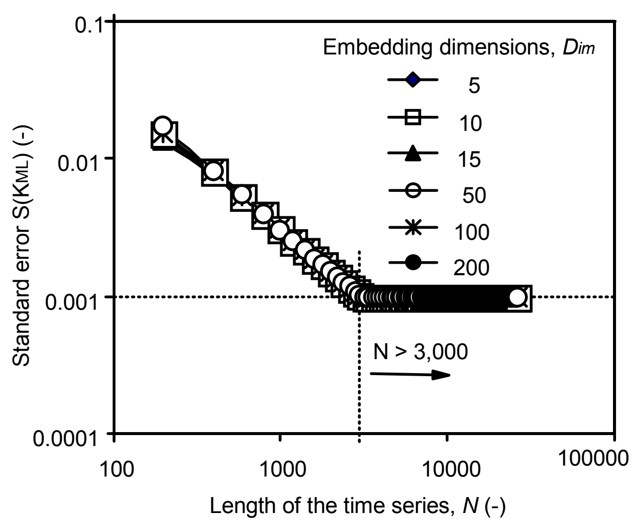

Figure 9: Effect of the time-series length on the accuracy of K_{ML} values (based on the standard error values), signal from a high-density riser

A semi-log plot of $M^{-0.5}$ versus K_{ML} is given in Figure 10. In this case, the number of data points was fixed, and then several values of K_{ML} were determined for each signal, from which the values of M (i.e. the number of crossings or the number of b values) were also computed. Throughout the downer, the values of $M^{-0.5}$ ranged only between 0.10% and 0.25% for all operating conditions. This range is sufficiently small for experimental signals. Moreover, the higher K_{ML} were determined at higher accuracy than the lower values. Compared to Figure 6, it implies that higher sampling frequencies from multiphase reactors lead to higher K_{ML} values and also to higher accuracy in the computation of K_{ML}.

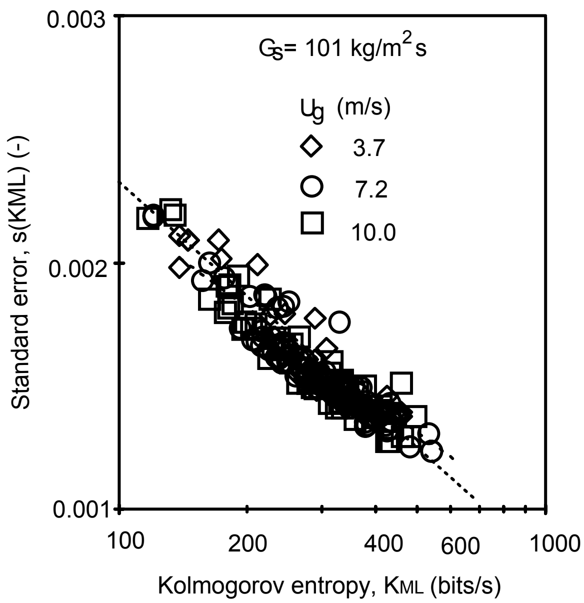

Figure 10: Standard error for the estimated values of entropy, $s(K_{ML})$, for signals from downer reactor operated at different gas velocities

The Effect of Jump-length for restarting a cont of b-values on a reconstructed vector

The number of points to be jumped, J_m, while looking for an arbitrary point to re-start counting the value of *b*, was not specified by Schoulten *et al.* (1994). How J_m affects K_{ML}, *b* and the standard error for estimation of K_{ML} is subject to analysis for experimental data, which has not been done using experimental data from multiphase reactors. Figure 11 shows the effect of increasing J_m on K_{ML} for different number of embedding dimensions, D_{im}.

The effect of J_m on K_{ML} strongly depends on the number of embedding dimensions, D_{im}. At higher D_{im}, lower values of K_{ML} were observed. Thus, changing J_m changes the value of K_{ML}. For experimental data from multiphase reactors, it is recommended to fix the value of J_m throughout the analysis, preferably in the range of 150 - 350, when the K_{ML} curves become closer to each other. Further analysis revealed that J_m have no effect on $\overline{b}$, standard deviation, $\sigma(b)$, Skewness, $S_k(b)$, and Kurtosis K_u(b), even when D_{im} was changed from 5 to 200.

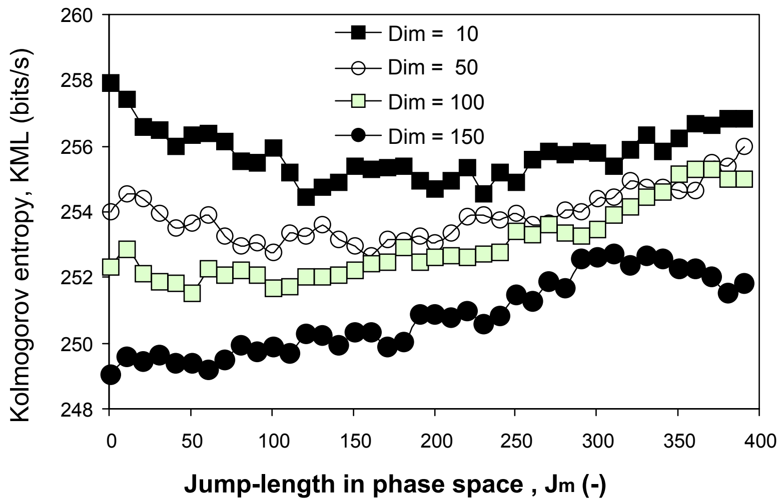

Figure 11: The effect of changing J_m on K_{ML}

Analysis of the Chaotic Behavior of the CFB using K_{ML}

After setting all the computational parameters to the optimum values (N, f, and J_m), according to the results of this analysis, the chaotic analysis of the CFB was investigated, based on the radial profiles, axial profiles and the effect of local solids concentration at different operating conditions. Figure 12 shows the effect of increasing ε_s on both K_{ML} in the fully developed-flow section (Z = 6.34) for a wide range of operating conditions in a high flux riser.

Increasing ε_s generally lowers K_{ML} for all operating conditions. Similar observation can be deduced from Figure 12, when G_s is increased from 300 to 550 kg/m^{2}s at constant gas velocity of 8.0 m/s. However, at constant G_s, the variation of K_{ML} with U_g is not clear. Using pressure fluctuations, Manyele *et al.* (2002a) reported the decrease of K_{ML} with G_s at constant U_g and also a decrease of K_{ML} as the apparent solids concentration were increased for all operating conditions. However, the effect of U_g was not elucidated.

The decrease in K_{ML} as G_s or ε_s is increased can be attributed to the increased cluster existence time and a decrease in cluster frequency at higher ε_s (Manyele *et al*., 2002; Soong *et al*., 1995; 1994) leading to extended time scales for changes in ε_s with time, such that the time scales predicted by K_{ML} becomes longer and hence lower K_{ML} values are observed. Longer time scales in the signal imply higher b-values and hence lower K_{ML}. On the reconstructed attractor, the number of points counted before the separation distance exceeds *AAD* becomes higher. In other words, the gas-solids flow stays longer in one dynamic state before it changes into another. Such a system is said to be easily predictable (relatively), attains low rate of information loss and it looses sensitivity to the disturbances.

The effect of increasing ε_s on K_{ML} was also studied at different axial elevations in a high flux riser. Figure 13 shows the variation of K_{ML} with ε_s at different axial elevations. Along the axial direction, the time scales are different due to several factors. At the bottom, due to the distributor effect (strong gas jets) and solids recirculation, K_{ML} is higher even at higher ε_s, as shown in Figure 13, which is in accordance to the fact that faster changes take place in the gas-solids flow in this section. In such a section the gas-solids flow is not easily predictable.

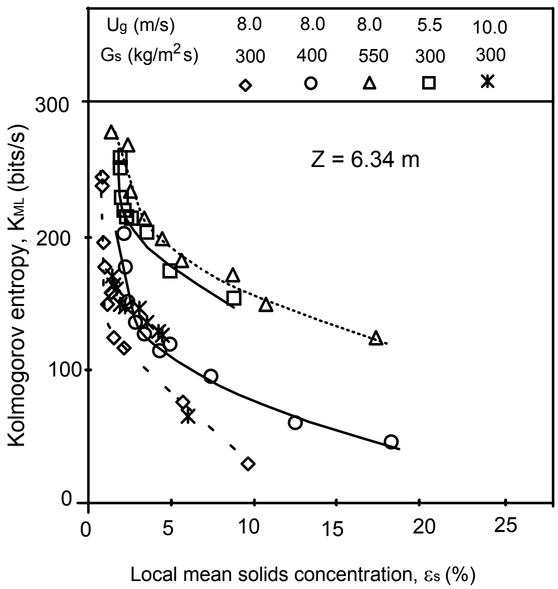

Figure 12: Variation of Kolmogorov entropy with local time-averaged solids concentration in the fully developed section of a high flux riser (Z = 6.34 m)

In the fully developed section, Z = 6.34 and 8.74 m, there is minimal wall effect, no solids acceleration, such that the time scales are longer than in the bottom. This leads to longer average cycle times (Manyele *et al*., 2002b) and hence lower K_{ML} values at comparable values of ε_s.

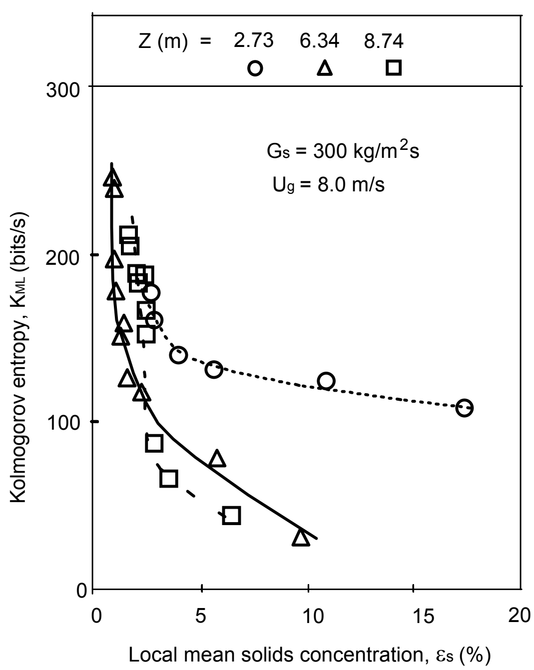

Figure 13: Variation of Kolmogorov entropy with local time-averaged solids concentration in different sections of a high flux riser

CONCLUSIONS

It can be concluded from this study that:

1) The measurements of solids concentration using a fiber optic probe are highly accurate with SNR of about 750 to 2000 and *CV* ranging from 30 to 80%.
2) The Skewness and Kurtosis of the solids concentration signals revealed that the properties of the PDF are accurately determined for the signals sampled at a frequency of 970 Hz and a duration of 30 seconds, which gives N = 27,000, and $S_{k,N}$ and $K_{u,N}$ well above 0.024 and 0.060, respectively, for a normal distribution.
3) The Skewness and Kurtosis of *b*-values ranged between 2.0 to 3.0 and 8.0 to 11.0, respectively, being well above the $S_{k,N}$ and $K_{u,N}$ for a normal distribution (using $N = 10^6$).
4) The K_{ML} is strongly affected by the sampling frequency of the signal from the multiphase reactor, which leads to different values reported in the literature for CFBs. Higher frequency leads to higher values of K_{ML} and vice versa.
5) The values of K_{ML} strongly depend on the length of the time series, N. For N< 1,000 points, the K_{ML} values depends strongly on the number of embedding dimension, Dim, while the latter was observed to have no effect for N > 1,000 points.
6) The standard error, $s(K_{ML})$, decreases to a constant minimum at 0.001, for N > 3,000 points. The effect of D_{im} is negligible on the $s(K_{ML})$. Higher values of K_{ML} are accurately determined than lower values, whereby $s(K_{ML})$ decreases with increasing K_{ML} value.
7) The K_{ML} decreases with increasing time-averaged solids concentration in the riser, due to corresponding longer time scales at higher ε_s. This was observed for all operating conditions and for all axial elevations.
8) The K_{ML} is a powerful tool for studying the dynamics of CFB reactors using chaos analysis. It can be used accurately for N > 3,000 data points. Higher values of N will lead to longer computations time.

NOMENCLATURE

AAD	Average absolute deviation (-)
b	number of steps before the separation distance exceeds AAD
CV	Coefficient of variation (%)
D_{im}	Number of embedding dimensions (-)
f	Sampling frequency (Hz)
G_s	Solids flux (kg/m^{2}s)
J_m	Number of points jumped to start a new counting of b values (-)
K_{ML}	Kolmogorov entropy determined by maximum likelihood method, (bits/s).
K_u	Kurtosis (-)
$K_{u,N}$	Kurtosis of a normal distribution
M	Number of b-values
N	Number of data points of original times series used for reconstruction of multidimensional vector (-)
$s(K_{ML})$	Standard error of the computed K_{ML}
S_k	Skewness (-)
$S_{k,N}$	Skewness of a normal distribution (-)
S*NR*	Signal-to-noise ratio (-)
U_g	Superficial gas velocity (m/s)

Greek letters

ε_s	Time –averaged solids concentration (%)
Δt	Sampling time interval (s)

REFERENCES

Addison, P.S., (1997), "Fractals and Chaos: An Illustrated Course", Institute of Physics Publishing (IOP) Ltd., Bristol, pp. 117-190.

Bai, D., Issangya, A.S., and Grace, J.R., (1999), "Characteristics of Gas-Fluidized Beds in Different Flow Regimes", *Ind. Eng. Chem. Res*., **38**, 803-811.

Cheng, Y.; Wei, F.; Lin, Q.; Jin, Y. A., (1998), Comparison of Local Chaotic Behaviors in a Riser and a Downer. In *Fluidization IX*. Fan, L.-S.; Knowlton, T.M., Eds.; Engineering Foundation, NY, , pp 613-620.

Daw, C.S., and Halow, J.S., (1991), "Characterization of Voidage and Pressure Signals from Fluidized Beds Using Deterministic Chaos Theory", Proc. of 11th Fluidized Bed Combustion (Ed. E.J. Anthony), ASME, **Vol. 2**, 777-786.

Daw, C.S., and Halow, J.S., (1992), "Modeling Deterministic Chaos in Gas Fluidized Beds", *AIChE Symp. Ser.* **88** (289), 61-69.

Daw, C.S., Lawkins, W.F., Downing D.J., and Clapp, Jr., N.E., (1990), "Chaotic Characteristics of a Complex Gas –Solids Flow", *Phys. Rev. A*, **41**(2), 1179-1181.

Finney, C.E.A, Kennel, M.B., Daw, C.S., and Halow, J.S., (1996), "Non-Linear Time Series Diagnostics of Fluidization Quality", *AIChE Annual Meeting*, Paper 188C, November 14,

Fuller, T.A., Flynn, T.J., and Daw, C.S., (1996), "Analysis of Dynamic Boiler Measurements: A Practical Approach", *Chem. Eng. J*., **64**, 179-189.

Grasberger, P., and Procaccia, I., (1983), "Estimation of the Kolmogorov Entropy from a Strange Signal", *Physcal Review*, **A28**, 2591-2594.

Hegger, R., Kantz, H. and Screiber, T., (1999), "Practical Implementation of Nonlinear Time Series Methods: The TISEAN Package, *Chaos*, **9**, 413.

Hoyer, D., Bauer, R., Walter B., and Zwiener, U., (1998), "Estimation of Nonlinear Couplings on the Basis of Complexity and Predictability – A New Method Applied to Cardiotherapy Coordination", *IEE Transactions on Biomedical Engineering*, **45**(5), 545-552

Johnson, H., and Johnson, F., (2001), "Measurement of Local Solids Volume Fraction in Fluidized Bed Boilers", *Powder Technol*., **115**, 13-26.

Manyele, S.V., Pärssinen J., and Zhu, J.-X., (2002b), "Characterizing Particle Aggregates in a Riser Operated at High Solids Flux", *Chemical Engineering J*., **88**, 151-161.

Manyele, S.V., Zhu, J.-X, Khayat, R.E., and Pärssinen, J., (2006), "Analysis of the Chaotic Dynamics of a High-Flux CFB Riser using Solids Concentration", *China Particuology*, Vol. **88 Nos. 3-4**, 136-146

Manyele, S.V., Zhu, J.-X., and Zhang, H., "Analysis of the Microscopic Flow Structure of a CFB Downer Reactor Using Solids Concentration Signal", *International Journal of Chemical Reactor Engineering,* **Volume 1**, Article A55, *Produced by The Berkeley Electronic Press*, 2003, pp. 1-17,

Manyele, S.V., Khayat, R.E., and Zhu. J., (2002a), "Investigation of the Dynamics of a High-flux CFB Riser Using Chaos Analysis of Pressure Fluctuations". *Chem. Eng. Technology*, **25**, 1-10.

Marzochella, A., Zijeveld, R.C., Schoulten, J.C., and van den Bleek, C.M., (1997), "Chaotic Behaviour of Gas-Solid Flow in the Riser of a Laboratory-Scale Circulating Fluidized Bed", AIChE J., 43, 1458-1468.

Müuller, U.A., Dacorogna, M.M., Davé, R.D., Pictet, O.V., Olsen, R.B., and Ward, J.R., (1995), "Fractals and Intrinsic Time- A Challenge to Econometricians", 34th In. Conf. of Applied Econometrics Association (AEA), Luxenbourg, 14-15 October, 1995.

Schaffer, W.M., (1985), "Can Nonlinear Dynamics Elucidate Mechanisms in Ecology and Epidermiology?", *IMA J. Math. Applied in Medicine & Biology*, **2**, 221-252.

Schoulten , J.C., and van den Bleek, C.M., (1998), "Monitoring the Quality of Fluidization Using the Short-term Predictability of Pressure Fluctuations", *AIChE J.*, **44**(1), 48-60.

Schoulten, J.C., Takens F., and van den Bleek, C.M., (1994) "Maximum Likelihood Estimation of the Entropy of an Attractor", *Physical Review E*, **49**(1), 126-129.

Soong, C. H., Tuzla, K., and Chen, J.C., (1994), "Identification of Particle Clusters in Circulating Fluidized Bed", in "Circulating Fluidized Bed Technology IV", A. A. Avidan, (Ed.), *AIChE*, New York, pp. 615-620.

Soong, C. H., Tuzla, K., and Chen, J.C., (1995), "Experimental Determination of Cluster Size and Velocity in Circulating Fluidized Bed", in "*Fluidization VIII*", J-F. Large and C. Laguerie (eds.), *Engineering Foundation*, New York, pp. 219-227.

van der Stappen M.L.M., Schoulten, J.C., and van den Bleek, C.M., (1993a), "Application of Deterministic Chaos Theory in Understanding the Fluid Dynamic Behavior of Gas-Solids Fluidization", *AIChE Symposium Series*, **89** (296), 91-102.

van der Stappen, M.L.M., Schoulten, J.C., and van den Bleek, C.M., (1993b), "Applications of Deterministic Chaos Analysis to Pressure Fluctuations Measurements in a 0.96-m^2 CFB Riser", *CFB IV Conference,* pp. 55-60.

Zhang, H., Johnson, P.M., Zhu, J.-X., de Lasa, H.I., and Bergougnou, M.A., (1998). "A Novel Calibration Procedure for an Optical Fiber Concentration Probe", *Powder Technol.*, **100**, 260-272.